



Research Article

Optimization of air inlet features of an active indirect mode solar dryer: A response surface approach

Promise Joseph ETIM^{a*}, Olalade MOSES OLATUNJI^a, Inemesit EDEM EKOP^a,
Akindele FOLARIN ALONGE^d, Ubong David OFFIONG^c, Kingsley Charles UMANI^{a,b*}

^aDepartment of Agricultural Engineering, Akwa Ibom State University, Ikot Akpaden, Nigeria

^bDepartment of Biological System Engineering, Washington State University, Pullman, USA

^cDepartment of Agricultural Engineering, University Putra, Malaysia

^dDepartment of Agricultural and Food Engineering, University of Uyo, Uyo, Nigeria

ARTICLE INFO

Article history

Received: 21 December, 2022

Revised: 22 January, 2023

Accepted: 22 February, 2023

Key words:

Air Flow Rate, Air Vent, Force of Drag, Optimization, Solar Dryer, Slice thickness

ABSTRACT

The effect of air flowing into an in an active indirect mode solar dryer was studied. The study aimed at optimizing the airflow features of a solar dryer of active indirect feature using Response Surface Methodology (RSM). The factors of the experiment included the product slice thickness of the experimental product and the air vent of the dryer. The two factors were considered at five levels and a total of 13 experimental runs derived. The air vent was based on the following shape orientations: square, rectangular, circular, and triangular. The thickness of the product was considered at five levels of 4, 8, 12, 16 and 20 mm. The responses from the experimental set up were the air flow rate and drag force, which were determined using established equations. The optimum values for the air flow rate and drag force were 0.0275 m³/s and 0.0476N, respectively. The corresponding optimal conditions which gave the optimum responses were 100 cm² - square inlet and product slice thickness of 20 mm for air flow rate and 80 cm² - rectangular inlet and product slice thickness of 20 mm for drag force, respectively. The models for predicting the responses were adequate, with r-square values 0.9463 and 0.9376 and desirabilities of 99.2 and 95.0% for air flow rate and drag force respectively. The experiment was repeated using the optimal conditions to validate the optimum responses. The variation between the predicted and experimental data was less than 8%.

Cite this article as: Etim PJ, Moses Olatunji O, Edem Ekop I, Folarin Alonge A, Offiong UD, Umani KC. Optimization of air inlet features of an active indirect mode solar dryer: A response surface approach. Clean Energy Technol J 2023;1:1:12–22.

*Corresponding author.

*E-mail address: promisetim@aksu.edu.ng



1. INTRODUCTION

The airflow into a solar drying system is a critical factor when increased quantity moisture is to be removed from the product, especially within first few hours of the drying [1, 2]. Most researchers do not consider the design of the air vent and its orientation as significant, as most of them rely on works of literature or assume values and make use of it.

Itodo et al. [3] highlighted the need for prior attention be paid to the air vent in the design of solar dryers, as it could have some effect on the volumetric airflow and performance. The study was borne out of the need to investigate if the air flowing into the air vent has any sort of effect on the process of drying.

Several researchers have deployed response surface methodology in optimizing solar drying systems, including but not limited to Erbay and Icier [4]; Majdi et al. [5]; Adefemi and Ilesanmi [6]; Zhanyong et al. [7]; Mohammed et al. [8]; Madamba [9]; Sarimenseli and Yaldiz [10]; Abano et al. [11]; Patil et al. [12]; Surki et al. [13] and Gupta et al. [14]. Adeyanju et al. [15] while determining the optimum conditions for deep fate drying of plantain, used response surface methodology and reported that the process could be better with the optimal conditions. Smitabhindu et al. [16] optimized the solar drying process for banana.

In optimizing the drying process for Moringa seed, Omofoyewa et al. [17] deployed the optimization method proposed by Box Behken and observed that the models developed predict about 70% of the responses.

Ikrang and Umani [18] optimized the drying process of catfish and observed that the different product sizes were affected by different conditions of drying. A similar report was also given by some researchers [19]. They reported that using RSM helped in reducing experimental runs, which they posited could be of huge benefit economically to researchers. Etim et al. [20] used RSM for optimization of the solar drying process for cooking banana.

This study aimed at optimizing the air inlet features (air flow into the dryer and force of drag) of an active indirect solar dryer to obtain optimum air inlet area for the solar dryer and examine the effect of the factors on the process of drying.

2. MATERIALS AND METHODS

The methodology involved computation of the air vent area and drag force using established equations. The independent factors (air vent area and the product slice thickness) were used to evaluate the optimal responses.

2.1. Air Inlet Area

The area of the square inlet vent was calculated using equation 1:

$$A_s = L \times B \quad (1)$$

Where A_s - the area of the square shaped air inlet (cm^2),

Highlights

- The airflow rate increases with the air vent area
- The air flow rate influences dryer performance
- Product thickness and air flow rate influences moisture removal
- Appropriate model selection helps in predicting desired responses

L - the length of the inlet(cm) and

B - the breath of the inlet (cm).

The area of the rectangular inlet vent was computed using equation 2:

$$A_r = L \times W \quad (2)$$

Where A_r - the area of the rectangular shaped air inlet (cm^2), L - the length of the inlet (cm) and W - the height of the inlet (cm).

The area of the circular inlet vent was computed using equation 3:

$$A_c = \pi r^2 \quad (3)$$

Where A_c - the area of the circular shaped air inlet (cm^2) and r - the radius of the inlet(cm).

The area of the triangular inlet vent was computed using equation 4:

$$A_t = 1/2 B \times H \quad (4)$$

Where A_t - the area of the triangular shaped air inlet (cm^2), B - the base of the inlet (cm) and H is the height of the inlet(cm).

2.2. Volumetric Air Flow Rate

The air flowing into the dryer was determined using equation 5:

$$\text{Air flow rate, } Q = AV \text{ (} m^3/s \text{)} \quad (5)$$

Where Q - Volumetric air flow rate, A - the area of inlet (m^2) and V - air flow velocity (m/s).

2.3. Drag Force

The force of drag was determined using equation 6:

$$F_D = 0.5 \rho V^2 A C_d \text{ (N)} \quad (6)$$

Where F_D - Drag force (N) is, ρ - Air Density (1.225 kg/m^3), V - Air Velocity (m/s), A - Air flow rate and C_d - Coefficient of drag (Dimensionless).

2.4. Experimental Design and Statistical Analysis

The independent factors were the air inlet area and the product slice thickness. The experiment was designed using RSM based on two factors and five levels. The technique was also used by Taheri-Garavand et al. [21] while optimizing the process of drying banana. Ndukwu et al. [22] also used similar method. A total of 13 experiments were outlined for each of the air vent shape considered. The experiment was repeated thrice, and the average obtained was used as a reference value for the respective factors.

The total number of treatment combination obtained using equation 7:

$$n = 2^k (n_p) + 2k (n_a) + k (n_c) \quad (7)$$

where k - number of independent variables, n - number of experiment repetitions at the center point; N_a , N_c , and N_f - the axial, central, and factorial points, respectively. The total number of design points was obtained using equation 8:

$$N = 2^k + 2k + (n_0) \tag{8}$$

The design gave a total of 13 experiments, 22 factorial points, eight axial points ($\alpha = 2$) and five replications. The coded value of the independent variables computed using equation 9:

$$\text{Coded value} = \frac{\text{Natural value - Baselevel (level 0)}}{\text{Interval of variation}} \tag{9}$$

The coded values were computed using the equation 10:

$$A_2 = (\text{PS} - 12) / 4 \tag{10}$$

A_2 = Coded value for slice thickness

PS = Natural value for slice thickness

The coded values were given as -2, -1, 0, 1, and 2, where -2, 0, and 2 represented the least, medium, and highest level respectively. The coded and actual values were contained in Table 1.

The response function Y was obtained from the equation below:

$$Y = \beta_0 + \sum_{i=1}^2 \beta_i X_i + \sum_{i=1}^2 \beta_{ii} X_i^2 + \sum_{i=1}^2 \sum_{j=i+1}^2 \beta_{ij} X_i X_j \tag{11}$$

Where: Y - response; β_0 - the constant coefficient; $\sum_{i=1}^2 \beta_i$ - the summation of coefficient of linear terms; $\sum_{i=1}^2 \beta_{ii}$ - summation of quadratic terms; $\sum_{i=1}^2 \sum_{j=i+1}^2 \beta_{ij}$ - the summation of coefficient of interaction terms; X_i , X_j are the independent variables.

2.5. Experimental Procedure and Data Collection

The dryers were subjected to tests at different levels, according to the factor's combination of the experiments, as shown in Table 2. A Lutron 4 in-1 digital meter (LM-8100), with a measurement range of 0.4 to 30.0m/s, was used to measure airflow velocity into the dryers on two hourly intervals. The data obtained was utilized for the computation of the air into the dryer. The airflow rate was the primary parameter for calculating the force each inlet could drag to enhance the drying process. The experiment was conducted three times using an active indirect solar dryer connected to a DC battery, which powered the blowers as in Figure 1. The dried samples (wrapped on a transparent polyethene) after the drying experiment is as captured in Figure 2.



Figure 1. Experimental set up.



Figure 2. Dried products after an experiment.

Table 1. Levels, Codes, and Intervals of Independent Variables for square shaped air inlet

Factors	Codes	Level				
		-2	-1	0	1	2
Product Slice Thickness (mm)	P	4	8	12	16	20
Air vent area (cm ²)						
Square shape	S	4	16	36	64	100
Rectangular shape	R	8	24	48	80	40
Circular shape	C	3.142	12.568	28.278	50.272	78.55
Triangular shape	T	8	16	24	32	40

Table 2. Experimental data for air flow rate and drag force of the dryer using square shaped air vent area and slice thickness

Run Order	Independent Factors			Responses											
	Air Vent Area (cm ²)	Slice thickness (mm)		Square Inlet			Rectangular Inlet			Circular Inlet			Triangular Inlet		
				Air Flow Rate (m ³ /s)	Drag Force (N)		Air Flow Rate (m ³ /s)	Drag Force (N)		Air Flow Rate (m ³ /s)	Drag Force (N)		Air Flow Rate (m ³ /s)	Drag Force (N)	
1	-2	0		0.0028	0.0008		0.0023	0.0041		0.0006	0.0007		0.0016	0.0021	
2	-1	-1		0.0059	0.0092		0.0064	0.0106		0.0029	0.0040		0.0050	0.0097	
3	-1	1		0.0053	0.0109		0.0058	0.0087		0.0037	0.0065		0.0047	0.0063	
4	0	-2		0.0091	0.0142		0.0142	0.0158		0.0076	0.0126		0.0063	0.0103	
5	0	0		0.0111	0.0213		0.0158	0.0322		0.0077	0.0127		0.0056	0.0081	
6	0	0		0.0130	0.0286		0.0152	0.0296		0.0094	0.0098		0.0065	0.0108	
7	0	0		0.0116	0.0231		0.0168	0.0362		0.0094	0.0194		0.0082	0.0181	
8	0	0		0.0118	0.0235		0.0160	0.0327		0.0076	0.0147		0.0064	0.0105	
9	0	0		0.0117	0.0212		0.0149	0.0285		0.0079	0.0130		0.0061	0.0095	
10	0	2		0.0119	0.0241		0.0134	0.0230		0.0101	0.0222		0.0063	0.0103	
11	1	-1		0.0181	0.0315		0.0235	0.0422		0.0158	0.0303		0.0080	0.0123	
12	1	1		0.0202	0.0394		0.0256	0.0502		0.0146	0.0260		0.0065	0.0081	
13	2	0		0.0240	0.0353		0.0097	0.0145		0.0144	0.0259		0.0123	0.0230	

2.6. Data Analysis

The significance of the model was determined using Analysis of Variance (ANOVA). It also showed the effect of each individual factor and how they interacted with the desired responses. The probability of error value (p-value) was used to check the significance of the respective coefficient of regression, which indicated the interaction effect.

Data obtained were analyzed to examine the significant difference in the responses and their interactions at a probability level of 5%. RSM plots were generated using a Design Expert (10.0.10) software package for designing experiments. Multiple regression equations were used to the relationship between the independent and dependent factors and test the fitness of the models in predicting the responses.

2.7. Response Optimization

The optimum values were obtained for the responses using numerical and graphical optimization technique to analyse the independent variables (air vent area and product slice thickness). RSM plots were used for the selection of the optimum combination of the independent variables to produce a model capable of predicting the desired responses. The range and optimization goals for the independent and dependent factors are as in Table 3.

3. RESULTS AND DISCUSSION

3.1. Model Selection for Optimization of Air Flow Rate (AFR) of an Active Indirect Mode Solar Dryer

The following models were selected: linear (square-shaped air vent), quadratic (rectangular-shaped air vent), linear (circular-shaped air vent), and linear (triangular-shaped air vent). The regression equations for the airflow rate with respect to dryers with square, rectangular, circular, and triangular vent were computed using equations 12 to 15.

$$AFR_{SQ} = 0.000284S_a + 0.000434P_s - 0.00000124S_a^2 - 0.000022 + 0.000000647S_aP_s - 0.00137 \quad (12)$$

$$AFR_{RE} = 0.000284R_a + 0.000247P_s - 0.000000368R_a^2 - 0.0000238P_s^2 + 0.00000651R_aP_s + 0.000951 \quad (13)$$

$$AFR_{CR} = 0.00429C_a + 0.000094P_s - 0.000541 \quad (14)$$

$$AFR_{TR} = 0.000272T_a - 0.00360P_s + 0.000347 \quad (15)$$

Where AFR_{SQ} , AFR_{RE} , AFR_{CR} and AFR_{TR} are respective air flow rates for air vents of square, rectangular, circular and triangular configurations

Table 3. Ranges and response goals for RSM optimization of the air flow properties

Response	Unit	Optimization Target (Goal)	Relative Importance
Air Flow Rate	m ³ /s	Maximize	Very important
Drag Force	N	Maximize	Very important

(m³/s); S_a , R_a , C_a and T_a , are respective areas of the square, rectangular, circular and triangular air vent (cm²); P_s is the slice thickness (mm).

Figures 3 to 6 show the relationship between air inlet areas, product sizes, and air flow rate variation. The air flowing into the dryer was dependent on the air vent area. This trend was like what was obtainable in the airflow rate.

The model p-value of < 0.0001 obtained for the square inlet dryer was less than the chosen significance level (0.05). It showed the significance of the model. The lack of fit p-value (0.0915) was higher than the significance level, as shown in Table 4.

The p-value for the square shape air inlet dimensions of 0.0001, was lower than the significance level (0.05), while the p-value of the slice thickness of 0.107, was higher than the level of significance. It meant that the inlet area significantly affected the airflow rate of the square-shaped vent dryers, while the product slice thickness had no significant effect. The model gave a high coefficient of determination ($R^2 = 0.9474$). The high R^2 value indicated that the model accounts for 94.74 % of the total variability in the response and that there is high correlation between the independent variables.

The favourable linear terms of equations 13 and 15 meant that air flow into the dryer increased as the air vent area increased. The favourable interaction terms suggested that an

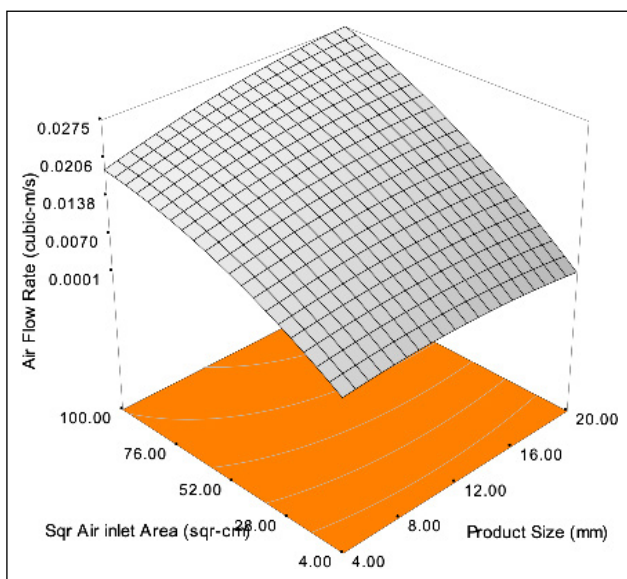


Figure 3. Response Surface plot of air vent area, air flow rate and Slice thickness for square air inlet.

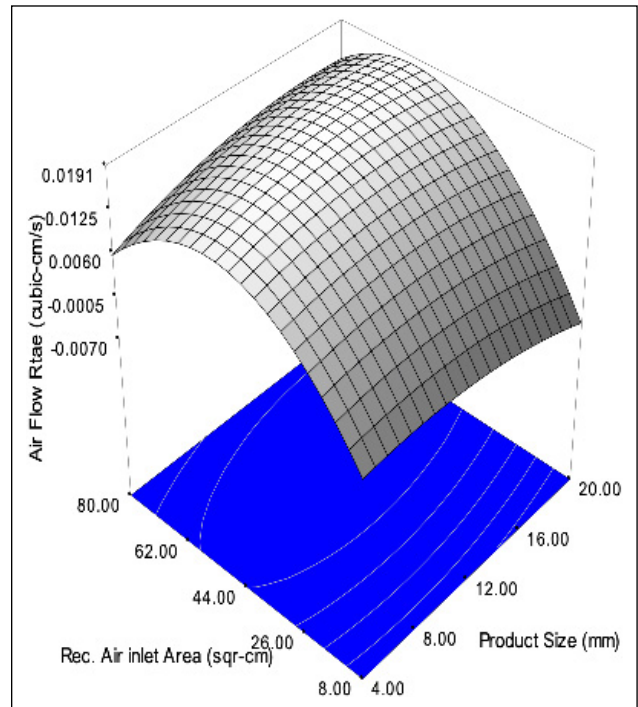


Figure 4. Response Surface plot of air inlet area, air vent rate and Slice thickness for rectangular air inlet.

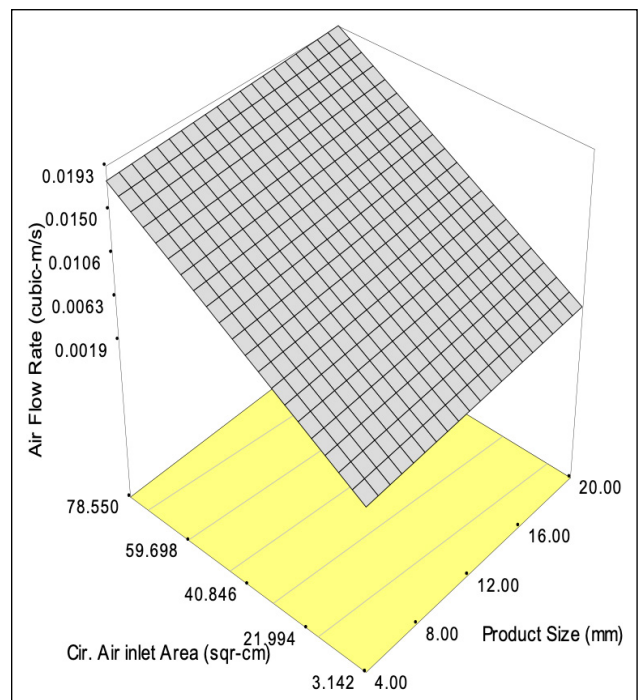


Figure 5. Response Surface plot of air vent area, air flow rate and Slice thickness for circular air inlet.

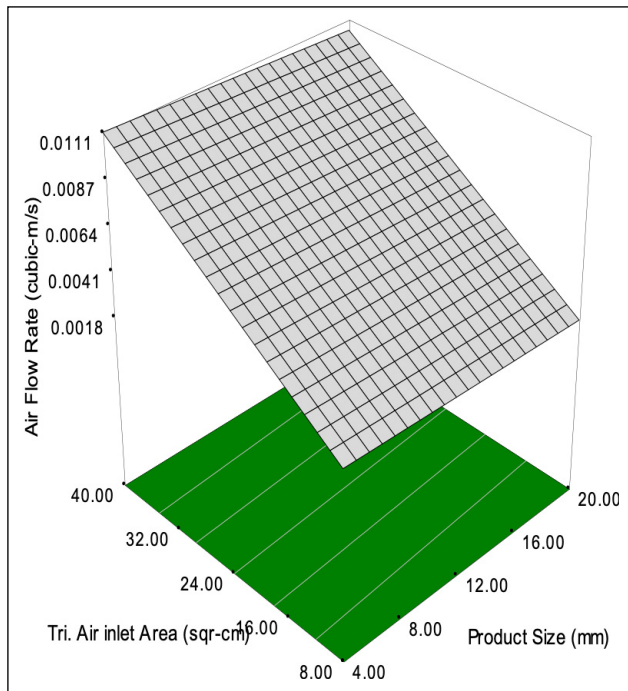


Figure 6. Response Surface plot of air inlet area, air vent rate and Slice thickness for triangular air inlet.

increase in the levels of the independent factors correspondingly increased the response. The response plots in Figures 3 to 6 were generated for best-fit as a function of the independent factors. The response was kept at its central point.

The airflow rate was observed to increase with increase in the air vent area. The slice thickness had no effect on the air flow into the dryer. Hedge et al. [23], Khaldi et al. [24], and Etim et al. [25] reported that an increase in the air vent area of a solar dryer enhances air flow into the dryer and efficiency.

3.2. Model Selection for Optimization of Drag Force (DF) of an Active Indirect Mode Solar Dryer

The models that were best fit for optimization of drag force were: quadratic (square-shaped air vent), quadratic (rectangular-shaped air vent), linear (circular-shaped air

vent), and linear (triangular-shaped air vent). The regression equations for the drag force of the dryer for the respective shape orientations were as given in equations 16, 17, 18, and 19.

$$DF_{SQ} = 1.58S_a P_s + 0.000779S_a + 0.00168P_s - 0.00000574S_a^2 - 0.00069P_s^2 - 0.01 \tag{16}$$

$$DF_{RE} = 0.00000216R_a P_s + 0.000491R_a + 0.00341P_s - 0.000000994R_a^2 - 0.000169P_s^2 - 0.02 \tag{17}$$

$$DF_{CR} = 0.00802C_a + 0.000362P_s - 0.01 \tag{18}$$

$$DF_{TR} = 0.000383T_a - 1.56P_s + 0.000977 \tag{19}$$

Where DF_{SQ} , DF_{RE} , DF_{CR} and DF_{TR} are respective drag force for air vents of square, rectangular, circular and triangular configurations (m^3/s); S_a , R_a , C_a and T_a , are respective areas of the square, rectangular, circular and triangular air vent (cm^2); P_s is the slice thickness (mm).

The RSM plots in Figures 7 to 10 show the relationship between air inlet areas, slice thickness, and drag force vari-

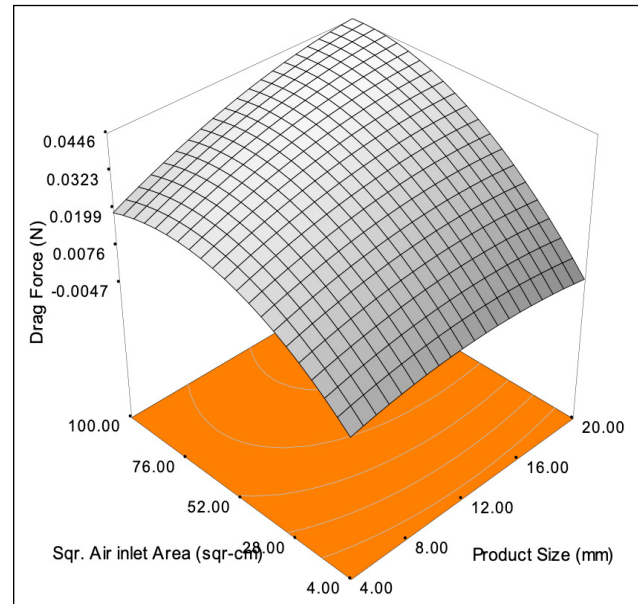


Figure 7. Response Surface plot of drag force, air flow rate and Slice thickness for square air inlet.

Table 4. Regression analysis of response surface quadratic model for air flow rate and drag force for Square Air Inlet Shape

Regression Terms	Air Flow Rate (Quadratic Model)	Drag Force (Quadratic Model)
Standard Deviation	0.0001.441	0.0036
Mean	0.012	0.022
Coefficient of Variation	11.97	16.32
Predicted Sum of Squares	0.00003779	0.00056
Coefficient of Determination (R^2)	0.9463	0.9376
Adjusted R^2	0.9414	0.8930
Predicted R^2	0.9112	0.6064
Adequate precision	40.99	16.53

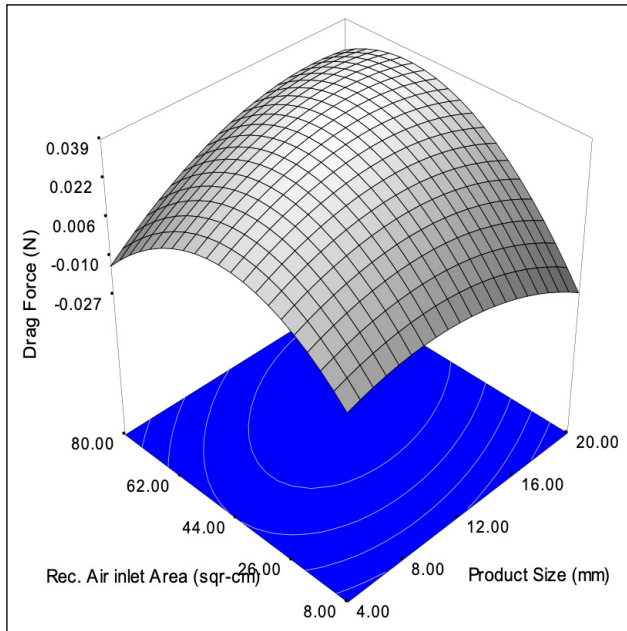


Figure 8. Response Surface plot of drag force, air flow rate and Slice thickness z_e for rectangular air inlet.

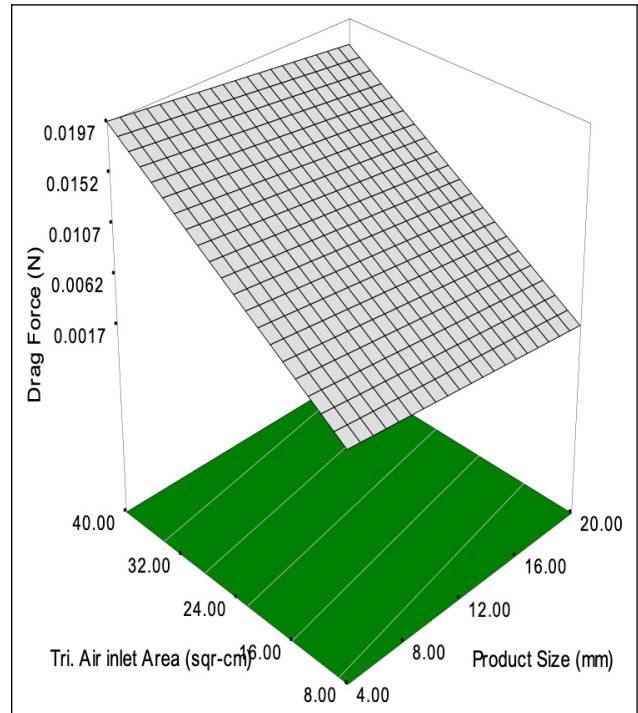


Figure 10. Response Surface plot of drag force, air flow rate and Slice thickness for triangular air inlet.

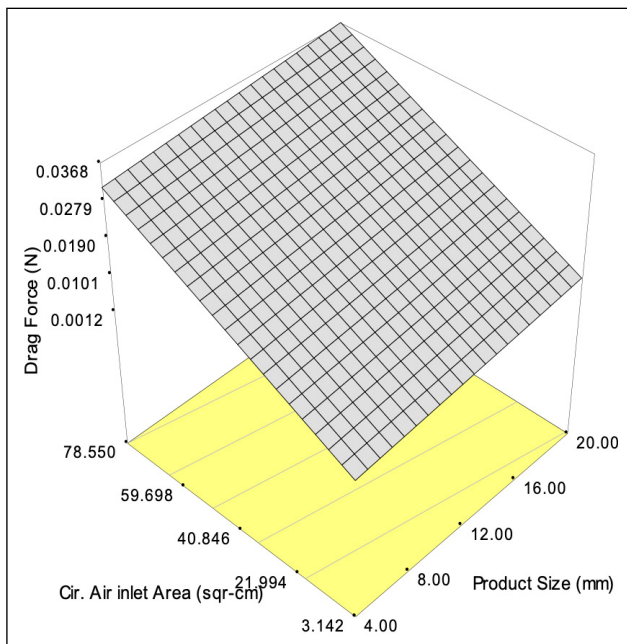


Figure 9. Response Surface plot of drag force, air flow rate and Slice thickness for circular air inlet.

ation. The force of drag was a function of the air inlet area. This trend was like what was obtainable in the airflow rate.

Table 5 shows the quadratic model ANOVA for the square-shaped air vent dryer, which had the highest coefficient of determination and least standard deviation.

The p-value of the model (0.0004) for the square-shaped vent dryers was lower than the desired significance level. The lack of fit p-value of 0.2684 was higher than the 5%

significance level. The model terms p – values were less than the significance level, as in Table 6. It meant that the terms of the model significantly affected the drag force. The coefficient of determination ($R^2 = 0.9376$) meant a positive correlation exist between the independent variables. The response model was responsible for 93.76% of the total variations in the response.

The positive linear term in equation 19 meant that the force of drag increased as the air vent area increased. The favourable interaction terms in equations 16 and 17 established that an increase in the independent factors correspondingly increased the drag force.

The RSM plots in Figures 7 to 10 were generated for the best-fit models as a function of the factors. The force of drag increased with an increase in the air vent area. The product slice thickness had no significant effect on the drag force. Etim et al. [26] posited that the airflow into the dryer greatly influences the force of drag of an active indirect mode solar dryer.

3.3. Optimization Goals

The desired goals for each drying parameter for the respective shape orientations are shown in Tables 7, 8, 9, and 10, respectively. To optimize the air flow rate and force of drag by numerical optimization, the equal importance of ‘3’ was given to the independent factors (air vent area and slice thickness) and the desired responses (air flow rate and drag force).

Table 5. ANOVA for RSM quadratic model for air flow rate of square shapes air inlet dryer

Source of Variation	Sum of Squares	df	Mean Square	F-Value	Prob> F
Model	0.0004170	5	0.00008340	68.18	< 0.0001
SAI	0.0004027	1	0.00040272	329.24	< 0.0001
PS	0.0000042	1	0.00000418	3.42	0.1070
SAI ²	0.0000036	1	0.00000357	2.92	0.1313
PS ²	0.0000024	1	0.00000241	1.97	0.2036
SAI×PS	0.0000018	1	0.00000179	1.46	0.2655
Residual	0.0000086	7	0.00000122		
Lack of Fit	0.0000066	3	0.00000220	4.46	0.0915
Pure Error	0.0000020	4	0.00000049		
Cor Total	0.0004256	12			

Where SAI represents Square Air Inlet, PS represents slice thickness.

The summary of the optimal air vent area and slice thickness and predicted optimum values for air flow rate and drag force were obtained as in Table 11.

3.4. Optimization and Validation of Air Flow Rate of an Active Indirect Mode Solar Dryer

The optimization process of the optimum value of the airflow rate of an active indirect mode solar dryer was performed. The result is shown in Table 11. The optimal values of 0.0275, 0.0250, 0.0179, and 0.0105 m³/s were obtained for square, rectangular, circular, and triangular-shaped air vent dryers that corresponded to the air vent area of 100 cm², 80 cm², 78.55 cm², and 40 cm² respectively. The corresponding optimal product size was 20 mm. The optimum air flow rate desirability was 0.992, 0.950, 1.000, and 0.895 for the respective air inlet shapes. Optimum values of 100 cm² (square air vent) and 20 mm (slice thickness) gave the maximum optimum air flow rate of 0.0275 m³/s and desirability of 99.2 %.

The optimal conditions of 100 cm² and 20 mm for air vent and slice thickness were used to validate the linear model of air flow rate for square air inlet dryers. The experimental data for the air flow rate obtained was 0.029 m³/s. The variation between the predicted value and the validated data obtained from the field after the test run was 0.0015 (5.17 %), as in Table 12.

The results for the predicted and experimental optimum air flow rate when compared showed a strong relationship between both sets of data. The variation between the predicted and the experimental value was relatively low, which suggested that the model can predict the air flow rate of an active indirect mode solar dryer.

3.5. Optimization and Validation of Drag Force of an Active Indirect Mode Solar Dryer

The optimum drag force of the dryers was determined. The result is shown in Table 11. Optimal values of 0.0445, 0.0476, 0.0341, and 0.0172 N were obtained with respect to

Table 6. ANOVA for RSM Quadratic Model for drag force of square shapes air inlet dryer

Source of Variation	Sum of Squares	df	Mean Square	F-Value	Prob> F
Model	0.001329	5	0.0002659	21.04	0.0004
SAI	0.001195	1	0.0011947	94.54	< 0.0001
PS	0.000072	1	0.0000720	5.70	0.0484
SAI ²	0.000041	1	0.0000412	3.26	0.1141
PS ²	0.000026	1	0.0000262	2.07	0.1934
SAI×PS	0.000010	1	0.0000096	0.76	0.4114
Residual	0.000088	7	0.0000126		
Lack of Fit	0.000052	3	0.0000174	1.92	0.2684
Pure Error	0.000036	4	0.0000091		
Cor Total	0.001418	12			

Where SAI represents Square Air Inlet, PS represents Slice thickness.

Table 7. Criteria and output for numerical optimization of square shaped air vent area of an active indirect mode solar dryer

Drying criteria	Unit	Lower limit	Upper limit	Optimization Goal	Relative Importance	Output
Sqr air inlet dim.	cm ²	4.00	100.00	Range	3	100.00
Slice thickness	mm	4.00	20.00	Range	3	20.00
Air Flow Rate	m ³ /s	0.00277	0.024	Maximize	3	0.0275
Drag Force	N	0.000827	0.0394	Maximize	3	0.0445
Desirability						0.992

Table 8. Criteria and output for numerical optimization of Rectangular shaped air vent area of an active indirect mode solar dryer

Drying criteria	Unit	Lower limit	Upper limit	Optimization Goal	Relative Importance	Output
Rec. air inlet dim.	cm ²	8.00	80.00	Range	3	80.00
Slice thickness	mm	4.00	20.00	Range	3	20.00
Air Flow Rate	m ³ /s	0.00232	0.0256	Maximize	3	0.0250
Drag Force	N	0.00412	0.0502	Maximize	3	0.0476
Desirability						0.950

Table 9. Criteria and output for numerical optimization of Circular shaped air vent area of an active indirect mode solar dryer

Drying criteria	Unit	Lower limit	Upper limit	Optimization Goal	Relative Importance	Output
Cir. air inlet dim.	cm ²	3.142	78.55	Range	3	78.55
Slice thickness	mm	4.00	20.00	Range	3	19.94
Air Flow Rate	m ³ /s	0.000577	0.0158	Maximize	3	0.0179
Drag Force	N	0.000653	0.0303	Maximize	3	0.0341
Desirability						1.000

Table 10. Criteria and output for numerical optimization of Triangular shaped air vent area of an active indirect mode solar dryer

Drying criteria	Unit	Lower limit	Upper limit	Optimization Goal	Relative Importance	Output
Tri. air inlet dim.	cm ²	8.00	40.00	Range	3	40.00
Slice thickness	mm	4.00	20.00	Range	3	20.00
Air Flow Rate	m ³ /s	0.00163	0.0123	Maximize	3	0.0105
Drag Force	N	0.00206	0.023	Maximize	3	0.0172
Desirability						0.895

Table 11. Optimal air vent area and slice thickness with optimum predicted responses

Air inlet shape	Drying process parameters		Optimum predicted responses		Desirability
	Air inlet area (cm ²)	PS (mm)	AFR (m ³ /s)	DF (N)	
Square	100.00	20.00	0.0275	0.0445	0.992
Rectangular	80.00	20.00	0.0250	0.0476	0.950
Circular	78.55	20.00	0.0179	0.0341	1.000
Triangular	40.00	20.00	0.0105	0.0172	0.895

PS is the Slice thickness, AFR is the Air Flow Rate, while DF is the Drag Force.

Table 12. Deviation in validation of optimum responses

Response	Optimum Value	Field Experiment	Deviation
Air Flow Rate (m ³ /s)	0.0275	0.029	0.0015 (5.17%)
Drag Force (N)	0.0476	0.0441	0.0035 (7.94%)

square, rectangular, circular, and triangular-shaped air vent dryers that corresponded to the air vent area of 100 cm², 80 cm², 78.55 cm², and 40 cm² respectively. The slice thickness that gave the optimum condition was 20 mm. The optimum drag force (0.0476N) was obtained from a rectangular inlet area of 80 cm², with a product size of 20mm at desirability of 95%. Like what was obtained for a flat plate collector type solar dryer [27].

The experiment was repeated using the optimal conditions of 80 cm² and 20 mm for air vent area and slice thickness for the validation of the model used. An experimental value of 0.0441 N was obtained. The result from the field based on the optimal values showed a deviation below 8% with the predicted value, as in Figure 11.

The predicted and experimental results for the drag force showed a strong relationship between both sets of data as in Figure 12. The lower deviation suggested that the model generated can predict the force of drag of an active indirect solar dryer for the given conditions.

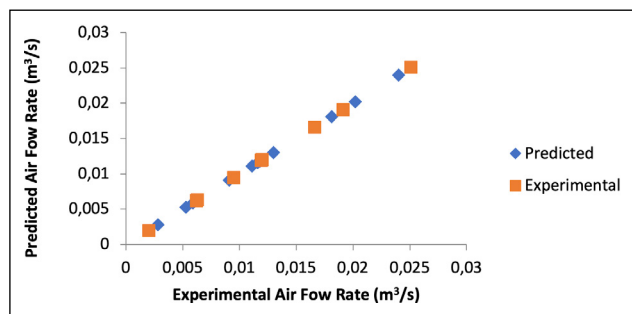


Figure 11. Predicted v Experimental: Air flow rate.

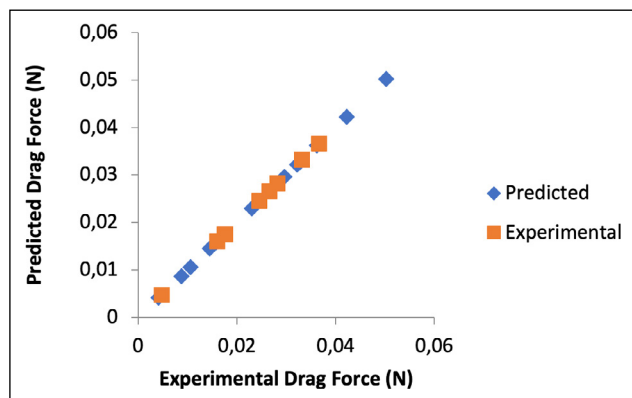


Figure 12. Predicted v Experimental: Drag Force.

4. CONCLUSIONS AND RECOMMENDATIONS

The RSM plots showed that the air vent area, air flow rate, and drag force were positively correlated. The models selected were able to predict the responses. The optimum responses obtained were 0.0275 m³/s and 0.0476 N for air flow rate and drag force, respectively. The corresponding dryers that gave the optimum responses were square (100 cm² air vent area) and rectangular (80 cm² air vent area), which were recommended for optimal air flow into an active indirect solar dryer for better performance. The desirability of the responses was 99.2 and 95% for air flow rate and drag force, respectively. It is recommended that the cross-sectional area (air vent area) be kept the same for the different inlet shapes to examine if such would affect air flowing into the dryer and overall performance of the dryer.

ACKNOWLEDGMENTS

The author acknowledges the contributions of the staff of the Department of Agricultural Engineering, Akwa Ibom State University.

AUTHORSHIP CONTRIBUTIONS

Authors equally contributed to this work

DATA AVAILABILITY STATEMENT

The authors confirm that the data that supports the findings of this study are available within the article. Raw data that support the finding of this study are available from the corresponding author, upon reasonable request.

CONFLICT OF INTEREST

The author declared no potential conflicts of interest with respect to the research, authorship, and/or publication of this article.

ETHICS

There are no ethical issues with the publication of this manuscript.

REFERENCES

[1] Alamu OJ, Nwakocho CN, Adunola O. Design and construction of a domestic passive solar food dryer.

- Leonardo J Sci 2010;16:71–82.
- [2] Oguntola JA, Colins NN, Olayinka A. Design and construction of a domestic passive solar food dryer. Leonardo J Sci 2010;16:23–30.
- [3] Itodo IN, Adewole AM, Edamaku SK. Development of an active solar crop dryer: Design analysis and performance evaluation. J Food Sci Technol 2004;41:37–42.
- [4] Erbay Z, Icier F. Optimization of Hot Air Drying of Olive Leaves using Response Surface Methodology. J Food Eng 2009;91:533–541. [CrossRef]
- [5] Majdi H, Esfahani JA, Mohebbi M. (2019). Optimization of convective drying by response surface methodology. Comput Electron Agric 2019;156:574–584. [CrossRef]
- [6] Adefemi AO, Ilesanmi DA. Development and optimization of drying parameters for low-cost hybrid solar dryer using response surface methodology. Sustain Bioenergy Syst 2018;8:23–35. [CrossRef]
- [7] Zhanyong G, Shaohua J, Ting J, Jinhui P, Libo L, Feng J. Optimization on Drying of Cucl Residue by Hot-Air Using Response Surface Methodology. Drying, Roasting and Calcining of Minerals. Berlin: Springer. p. 73–80. [CrossRef]
- [8] Mohammad JD, Seyed SM, Shanin R. Optimization on drying conditions of a solar electro-dynamic drying system based on desirability. Food Sci Nutrit 2014;2:758–767. [CrossRef]
- [9] Madamba, P. S. (2007). Optimization of the drying process: an application to the drying of garlic. Drying Technol 2007;15:117–136. [CrossRef]
- [10] Sarimeseli A, Yaldiz Z. Optimization of microwave drying of celery using response surface methodology. Focusing Modern Food Industry 2016;5:16–24.
- [11] Abano EE, Ma H, Qu W. Optimization of drying conditions of quality dried tomato slices. Food Process Preserv 2013;38:212–221. [CrossRef]
- [12] Patil BN, Gupta SV, Wakhande VR. Response surface methodology of osmotic dehydration of sapota slices. J Agric Food Sci Technol 2014;5:249–260.
- [13] Surki AA, Sharifzade F, Afshari T, Hosseini NM, Gazor HR. Optimization of processing parameters of soyabean seed dried in a constant bed dryer using response surface methodology. Agric Sci Technol 2012;12:409–423.
- [14] Gupta MK, Sehgal VK, Arora S. Optimization of drying process parameters for drying cauliflower. Food Sci Technol 2013;50:62–69. [CrossRef]
- [15] Adeyanju JA, Olajide JO, Adedeji AA. Development of optimum operating conditions for quality attributes in deep-fat frying of dodo produced from plantain using response surface methodology. Food Nutrit Sci 2016;7:1423–1433. [CrossRef]
- [16] Smithabhindu R, Janjal S, Chankong V. Optimization of solar assisted drying system for drying bananas. Renew Energy 2008;33:1523–1531. [CrossRef]
- [17] Omofoyewa MG. Optimization of drying parameters of moringa seed in a tray dryer using box-behnken technique of RSM. Sci Eng Res Africa 2017;32:86–99. [CrossRef]
- [18] Ikrang EG, Umani CK. Optimization of process conditions for drying of catfish (*Clarias Gariepinus*) using response surface methodology (RSM). Food Science and Human Wellness 2019;8:46–52. [CrossRef]
- [19] Sunil SN, Garg A, Kumar S. An overview of optimization techniques used in solar drying. Asian J Sci Appl Technol 2013;1:5–11.
- [20] Etim PJ, Eke AB, Simonyan KJ. Design and development of an active indirect solar dryer for cooking banana. Scientific African. 2020;8:e00463. [CrossRef]
- [21] Taheri-Garavand A, Karimi F, Karimi M, Lofti V, Khoobakht G. Hybrid response surface methodology artificial neural network optimization of drying process of banana slices in a forced convective dryer. Food Sci Technol Int 2017;24:277–291. [CrossRef]
- [22] Ndukwu MC, Ekop IE, Etim PJ, Ohakwe CN, Ezeji-for, N. R., Onwude, D. I., Abam, F. I., Igboayaka, E. C. and Ohia, A. Response surface optimization of Bambara nut kernel yield as affected by speed of rotation, and impeller configurations. Sci African 2019;6:e00174. [CrossRef]
- [23] Hedge VN, Hosur VS, Rathod SK, Harsour PA, Narayana KB. Design, fabrication, and performance evaluation of solar dryer for banana. Energy Sustain Soc 2015;5:1–12. [CrossRef]
- [24] Khaldi S, Korti AN, Abboudi S. Applying CFD for studying the dynamic and thermal behaviour of an indirect solar dryer: Parametric analysis. Mech Mech Eng 2018;22:253–272. [CrossRef]
- [25] Etim PJ, Eke AB, Simonyan KJ. Effect of air inlet duct features and grater thickness on cooking banana drying characteristics using active indirect mode solar dryer. Niger J Technol 2019;38:1056–1063. [CrossRef]
- [26] Etim PJ, Eke AB, Simonyan KJ. (2019). Effect of air inlet opening on air flow rate and drag force of an active indirect mode solar dryer. J Adv Eng Res Sci 2019;6:512–519. [CrossRef]
- [27] Eke AB, Etim PJ. Prediction of optimum tilt angle of Flat-plate solar collector in Abia State Nigeria. Int J Eng Innov Res 2022;4:143–153. [CrossRef]